

RECENT DEVELOPMENTS IN DESIGNS FOR e^+e^- COLLIDERS

K. Ohmi for the KEKB Commissioning Group
KEK, Oho, Tsukuba, 305-0801, Japan

Abstract

We discuss an design of future e^+e^- collider from the view point of the beam dynamics. The crossing angle permits short bunch spacing without complex design of the interaction region. In KEKB, the crossing angle did not degrade the collision performance. However we need to study how the crossing angle affects the beam-beam interaction for the future high luminosity colliders. The electron cloud instability, which limited the luminosity performance in positron ring, have been somehow recovered by using solenoid magnets. The ion instability, which have been observed in electron rings, may be serious for higher beam current. We have to study which particle should be stored in high or low energy rings to minimize the instability effects. The coherent synchrotron radiation becomes serious for short bunch length and high bunch current. We discuss these issues one by one.

INTRODUCTION

B factories in the world, PEP-II and KEKB, have been successfully operated with very high luminosities. The peak luminosities of PEP-II and KEKB are 0.61×10^{34} and $1.06 \times 10^{34} \text{ cm}^{-2}\text{s}^{-1}$, respectively, at May, 2003. The operations are somewhat different from their original designs. In the both factories, the number of bunches is less than the design values, and bunch current is higher than the design values. They are operated in a regime where beam-beam parameter is saturated ~ 0.05 .

We are challenging to get more luminosity everyday. The solenoid magnet coils to avoid the electron cloud effects were wound everywhere as possible as we could. The horizontal tune was controlled to keep closed to half integer. Vertical tune and chromaticity was scanned to get higher luminosity and useful beam life time every time. Geometrical condition of collision, offset of two beam, vertical crossing angle and RF phase were scanned and feed backed in every second. All of optics parameters at the collision point, $\beta_{x(y)}$ functions, dispersions ($\eta_{x(y)}$, $\eta'_{x(y)}$), x-y coupling parameters ($R_1 - R_4$) were scanned every time [1, 2].

In PEP-II, 945 bunches are stored with 6 ns spacing. In KEKB, 1000 bunches had been stored with 8 ns spacing, because increasing of the number of bunch did not contribute luminosity until last year (2002) perhaps due to electron cloud effects, not parasitic collision effects. As the result of addition of solenoid magnets in every long shut-down periods, the number of bunches can be made increase gradually. Attempt to increase the number of bunches has been continued in KEKB.

In the both of SLAC and KEK, upgrade plans toward the luminosity of $10^{35} - 10^{36} \text{ cm}^{-2}\text{s}^{-1}$ are proposed. We discuss the design development of the upgrade plan of KEKB, named by super KEKB, in this report. The parameters for the present operation of KEKB and those for the design of Super KEKB are shown in Table 1.

We discuss three topics: beam-beam effects, instabilities and coherent synchrotron radiation. Collision with/without a crossing angle is reviewed in Sec.II. Electron cloud and ion instabilities are discussed in Sec.III. These studies inform which particle stored in low energy or high energy rings. Longitudinal single bunch instability due to the coherent synchrotron radiation is discussed in Sec.IV.

CROSSING ANGLE

In high luminosity e^+e^- factories, KEKB and DAΦNE adopt collision with finite crossing angle, and PEP-II adopts head-on collision. Crossing angle makes easy a design of the interaction region for the narrow bunch spacing. However the crossing collision scheme had been considered to be a taboo, since the unsuccessful experience of DORIS in DESY. In KEK and INFN, many studies were performed to decide the adoption of the crossing collision scheme [3, 4, 5]. KEKB and PEP-II have achieved luminosities of 1.06×10^{34} and $0.61 \times 10^{34} \text{ cm}^{-2}\text{s}^{-1}$, respectively at May, 2003. The beam-beam parameters are 0.05 for KEKB, respectively. Consequently, the crossing angle does not affect the beam-beam performance in the region of the beam-beam parameter up to 0.05.

We now target higher luminosity, $L = 10^{35} \sim 10^{36} \text{ cm}^{-2}\text{s}^{-1}$. The beam-beam parameter should be higher to get the luminosity. We need to review the effect of crossing angle on the beam-beam interaction for a higher beam-beam parameter.

Collision with a half crossing angle of θ is equivalent to that between beams with z dependent dispersion ($\zeta_x = \theta$) at the interaction point [6]. Crab cavities generate the dispersion $\zeta_x(s)$. Matching the dispersion as $\zeta_x = -\theta$ at the interaction point, effects of the crossing angle are canceled [7].

We have studied the beam-beam effects using the weak-strong and strong-strong simulation methods [8]. In the weak-strong method, one beam is represented by macro-particles and another beam is represented by a fixed Gaussian charge distribution. In the strong-strong method, both beams are represented by many macro-particles, and their interactions are evaluated by the particle in cell method.

The weak-strong simulation is executed for 100 macro-particles and 10 or more longitudinal slices during 40,000

Table 1: Basic parameters of present KEKB and Super KEKB

	KEKB		Super KEKB	
	HER	LER	HER	LER
particle	e^-	e^+	e^\pm	e^\mp
C	3016 m		3016 m	
E	8 GeV	3.5 GeV	8 GeV	3.5 GeV
N_\pm	5.4×10^{10}	7.3×10^{10}		
N_{bunch}	1280		5000	
β_x/β_y	60 cm / 7 mm		15 cm / 3 mm	
ε_x	24 nm	18 nm	18 nm	
σ_z	7 mm		3.5 mm	
$\nu_x/\nu_y/\nu_s$	0.515/0.565/0.02		0.515/0.565/0.02	
τ_{xy}/T_0	4,000	4,000	4,000	4,000-8,000
θ_c	11 mrad		0 – 15 mrad	
$L(\text{cm}^{-2}\text{s}^{-1})$	1.06×10^{34}		$1 \times 10^{35} - 10^{36}$	

revolutions. The strong-strong simulation is executed for 100,000 macro-particles and 5 longitudinal slices during 20,000 revolutions.

We calculated the luminosity for various current keeping the transparency condition. Figure 1 shows the beam-beam tune shift which is estimated by the luminosity for the positron current, I_+ . Pictures (a) and (b) are given by the weak-strong, and (c) and (d) are by the strong-strong. The tune shift should linearly depends on I_+ , if there is no dynamical effect of the beam-beam interaction. In the weak-strong simulation, the tune shift linearly increases up to 0.25 for head-on collision, while it saturates around less than 0.08 for crossing angle 11 mrad. The tune shift is extremely high beyond all belief. We use operating tune which is close to half integer in horizontal as is operated in KEKB.

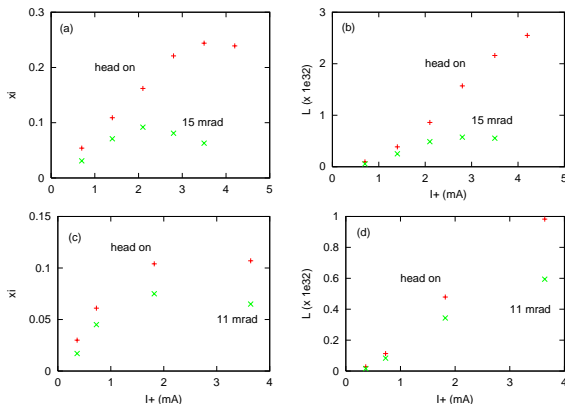


Figure 1: Beam-beam parameter (a)(c) and luminosity (b)(d) function of positron current for collisions with/without crossing angle. Pictures (a) and (b) are obtained by the weak-strong simulation, and (c) and (d) are by the strong-strong simulation.

Beam-beam halo is another limitation of the beam-beam effect [9]. The halo is evaluated by a very long term simulation using the weak-strong method. We used brute force simulation using 500 particle times 10^6 turn, though there is some technique to reduce the calculation time [9, 11]. The CPU time was a few 10 minute for 10 longitudinal slices. Figure 2 shows distribution of beam particles in $x - y$ plane. The particle times turn numbers, 5×10^8 , corresponds to more than 1 hour. Concerning also beam-beam halo, the head-on collision is better than that with finite crossing angle. [10].

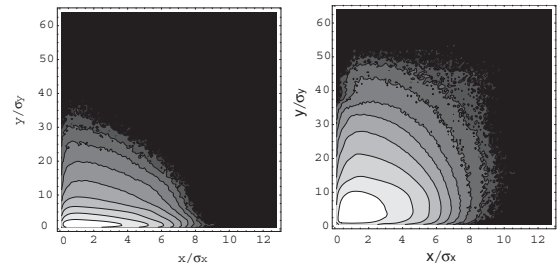


Figure 2: Beam-beam halo for collisions without (left) and with (right) crossing angle estimated by the weak-strong simulation.

PARTICLE AND ENERGY

In asymmetric B factories, PEP-II and KEKB, energies of electrons and positrons are chosen to be 8-9 GeV and 3-3.5 GeV. The choice is reasonable by considering an injector Linac, in which positrons are created as secondary particles by electrons accelerated to be several GeV. Electron beam can be accelerated to higher energy, while its intensity, which is primary, is stronger than that of positron beam.

From the viewpoint of the beam-beam interaction, the

number of particles with the low energy in a bunch is required to be more than those with the high energy. The so-called transparency condition is $N_H \gamma_H = N_L \gamma_L$, where $N_{H(L)}$ and $\gamma_{H(L)}$ are the number of particles and the relativistic factor of the high (low) energy, respectively. There is a merit to choose that electron beam has a lower energy.

In the B factories, ion and electron cloud instabilities are observed in electron and positron rings, respectively, and they affect the performances of the rings. We survey these instabilities and study which beam should have high or low energy.

Electron cloud effect

We first estimate build-up of an electron cloud for two case of the positron beam energies, $E = 3.5$ GeV and 8 GeV. The photoelectron instability model [12] is used for the estimation of the build-up. There are some codes to estimate the build-up [12, 13, 14]. We used the code PEI [12].

The primary electrons are created by synchrotron radiation with a production rate, $n_e = 0.0015/(\text{m}\cdot\text{e}^+)$, for a positron passage per a meter. This production rate corresponds that 100 photons create 1 photoelectron at the chamber surface. This is an empirical value for a test ante-chamber at KEKB. The photons are assumed to be created uniformly at the chamber.

The secondary yield is used a formula given by ref.[13],

$$Y_2(E) = Y_0 \exp(-5E/E_{max}) + Y_{max} \frac{E}{E_{max}} \frac{1.44}{0.44 + (E/E_{max})^{1.44}}. \quad (1)$$

$E_{max} = 200$ eV, $Y_0 = 0.5$ and $Y_{max} = 1.2$ are used here.

Figure 3 shows the electron cloud density for the beam energy of the cases of 3.5 GeV and 8 GeV. The density for 8 GeV is higher than that for 3.5 GeV: $\rho_e(8\text{GeV}) > \rho_e(3.5\text{GeV})$.

In a regime for a lower cloud density than neutralization, electrons are strongly overfocused by the beam, therefore cloud density is determined by dynamical balance of creation and absorption. In another regime for a high cloud density close to neutralization, the overfocusing force is weakened, therefore electrons tend to be accumulated up to the neutralization. If these two cases of 3.5 and 8 GeV are in the first regime, the cloud density of 8 GeV case should be more than that of 3.5 GeV: $\rho_e(8\text{GeV}) > \rho_e(3.5\text{GeV})$. Because the transparency condition, $N_H \gamma_H = N_L \gamma_L$, gives an equal number of photoelectrons production due to the number of photon scaling to $N_+ \gamma_+$, and the overfocusing force of low energy (high intensity) beam is stronger. If they are in the second regime, the electron line density is near the beam line density: that is, 3.5 GeV, which is higher line density, should be higher density, $\rho_e(8\text{GeV}) < \rho_e(3.5\text{GeV})$.

The simulation result in Figure 3, $\rho_e(8\text{GeV}) > \rho_e(3.5\text{GeV})$, shows that the both cases are in the first regime. The case of 8 GeV has so slow build-up time that it may be in

the second regime. Since these behaviors depend on parameters as electron production and secondary rates etc., we need more study whether these results are always obtained.

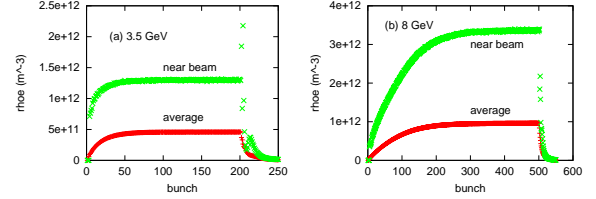


Figure 3: Electron cloud density for 3.5 GeV and 8 GeV cases.

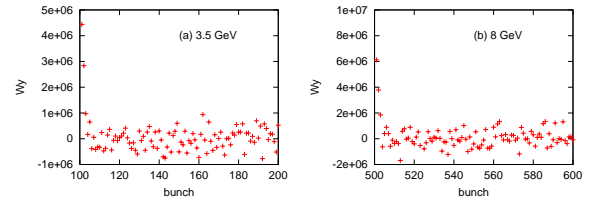


Figure 4: Wake field caused by the electron cloud for 3.5 GeV and 8 GeV cases.

We first estimate the coupled bunch instability caused by the electron cloud [12]. A bunch train which passes through the electron cloud experiences a wake force. Figure 4 shows the wake field for each case. The growth time can be estimated by the wake force induced by the electron cloud. The growth times were obtained as $\tau = 0.3T_0$ and $0.4T_0$ for the case of 8 GeV and 3.5 GeV, respectively. The growth time for 8 GeV was a little faster than that for 3.5 GeV. The strongest mode was around $m \approx 4500$, whose frequency was $\omega \approx (5120 - 4500)\omega_0 - \omega_\beta$ for either case. The growth rates are too fast to recover a bunch by bunch feedback system. Actually the electron cloud should be removed by solenoid magnets, ante-chamber, electrodes and other measures. We here focus the relative value of the growth: that is, 3.5 GeV is a little slower. This result may be due to that the cloud density for 3.5 GeV was further weaker, though the gamma factor is smaller.

We next study single bunch instability due to the electron cloud. The positron beam, which passes through the electron cloud, experiences a short range wake force. The wake force causes the strong head-tail instability. The instability can be simulated by some simulation codes [15, 16, 17, 18]. Figure 5 shows the growth of the vertical beam size for the cases of 3.5 and 8 GeV obtained by the code PEHTS [17].

The threshold of the strong head-tail instability due to the electron cloud is $\rho_{e,th} = 0.5 - 1 \times 10^{12} \text{ m}^{-3}$ for 3 GeV and $1 - 2 \times 10^{12} \text{ m}^{-3}$ for 8 GeV. The threshold densities for the cases of 3.5 and 8 GeV are about half of those estimated by the build up code in Figure 3. These results show that

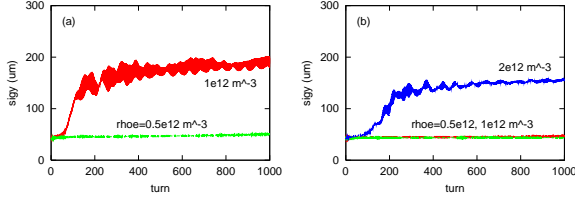


Figure 5: Growth of the single bunch instability caused by the electron cloud for (a) 3.5 GeV and (b) 8 GeV cases.

difficulties for the two cases are not big difference, because effect of γ is cancelled by the density difference.

Ion effect

We study which should choose 3.5 or 8 GeV for the electron beam energy. In an electron ring, ions, which produced by ionization of residual gas due to the beam, trapped in the bunch train, and causes a two-stream instability [19]. We studied this instability using a simulation model shown in Ref.[20, 21]. Electron bunch is assumed to be Gaussian distribution in the transverse plane and ions are represented by point-like macro-particles. In the simulation, the instability is caused by the oscillation of ions bounded in the bunch train. Ion species and yield are assumed as CO^+ and $4 \times 10^{-9}/(m \cdot e)$. This yield corresponds to the pressure of 1×10^{-7} Pa. Figure 6 shows growth of transverse amplitudes, $\sqrt{J_y(x)}$. Vertical growth is faster than horizontal

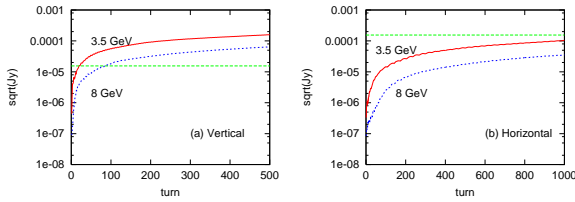


Figure 6: Growth of the fast ion instability. Blue and red lines are evolutions of $\sqrt{J_y(x)} m^{1/2}$ for $E = 8$ GeV and 3.5 GeV, respectively. Pictures (a) and (b) depict the vertical and horizontal growth, respectively.

one. The growth time is ~ 50 and < 10 turns for 8 GeV and 3.5 GeV cases, respectively. The growth time of each energy case is reasonable for the consideration of the γ factor and the beam line density. Perhaps growth time of 50 turn is limit for bunch by bunch feedback system. Concerning ion issue, the option of 8 GeV is better.

COHERENT SYNCHROTRON RADIATION

Bunch lengthening is important issue for keeping the length with high population. The threshold of longitudinal single bunch instability is discussed using Keil-Schnell-Boussard relation [22]. The impedance threshold value is

given by

$$|Z_{||}/n| = 0.66 Z_0 \frac{\alpha \gamma}{N_e r_e} \sigma_z^2 \sigma_z. \quad (2)$$

where $n = \omega/\omega_0$ and α is the momentum compaction factor. The threshold of the impedance Z/n is $\sim 0.05 \Omega$ for present KEKB.

Coherent synchrotron radiation affects the bunch lengthening [23, 24]. The wake force of the coherent radiation is given by [25, 26]

$$W_0(z) = \frac{2}{(3R^2)^{1/3}} \frac{\partial}{\partial z} z^{-1/3} \quad (3)$$

where R is the bending radius. The impedance integrated over the circumference is given as

$$Z_{||}(\omega) = \frac{i A Z_0}{2} \left(\frac{\omega R}{c} \right)^{1/3} \quad (4)$$

where $A = 3^{-1/3} \Gamma(2/3) (\sqrt{3}i - 1) = 1.63i - 0.94$. Since the impedance scales as $Z/n \propto \omega^{-2/3}$, the Keil-Schnell-Boussard criteria gives threshold frequency (ω_{th}) of the instability,

$$\omega_{th} R/c = 2.0 \Lambda^{3/2}, \quad (5)$$

where ¹

$$\Lambda = \frac{N_e r_e}{\alpha \gamma \sigma_\delta^2 \sqrt{2\pi} \sigma_z} \frac{R}{\bar{R}} \quad (6)$$

and $\bar{R} = L/2\pi = c/\omega_0$.

We have to consider that lower frequency component of the impedance, which satisfies a condition of $\omega \sigma_z/c < 1$, does not contribute the instability. The frequency component, which satisfies $\omega R/c > (\pi R/2b)^{3/2}$, is shielded by the chamber wall, where b is the chamber radius [27]. This gives another necessary condition for the instability, $b\Lambda/R > 1$.

The length of the bending magnet should be remember to be short for LER, $L_{\text{Bend}} = 0.76$ m [24]. If the correlation is determined by interaction in a bending magnet, the correlation length is estimated by the overtaking length for the radiation.

$$\ell_{\text{cor}} = \frac{1}{3R^2} \left(\frac{L_{\text{Bend}}}{2} \right)^3. \quad (7)$$

It is difficult to understand whether the synchrotron radiation emitted in a bending magnet affects the motion in another bending magnet. If it does not affect, the wake force should be truncated with the correlation length. Otherwise, a numerical simulation of motion, in which the correlation across bending magnets is included, should be performed [24].

These values for KEKB and super KEKB are summarized in Table 2.

¹The coefficient of $\Lambda^{3/2}$ was followed by Ref.[23].

Table 2: Coherent synchrotron radiation effect for KEKB and Super KEKB

	KEKB		Super KEKB	
	LER	HER	LER	HER
N_e	7.3×10^{10}	5.4×10^{10}	1.2×10^{11}	5.4×10^{11}
σ_z	5 mm	5 mm	3.5 mm	3.5 mm
α	10^{-4}	10^{-4}	10^{-4}	10^{-4}
σ_δ	7×10^{-4}	7×10^{-4}	7×10^{-4}	7×10^{-4}
Λ	1674	2905	4087	4150
ω_{th}	$2.5 \times 10^{12} \text{ s}^{-1}$	$1.1 \times 10^{12} \text{ s}^{-1}$	$8.9 \times 10^{12} \text{ s}^{-1}$	$2.2 \times 10^{13} \text{ s}^{-1}$
$\omega_{th}\sigma_z/c$	42	17	104	21
$b\Lambda/R$	5.1	1.7	11.9	2.4
L_{bend}	0.76 m	5.8 m	0.76 m	5.8 m
l_{cor}	69 μm	1 mm	69 μm	1 mm

SUMMARY

We discussed the design development of future B factories based on parameters of Super KEKB concerning the three issues (1) beam-beam effect with/without crossing angle, (2) energy choice, electron cloud and ion instabilities, and (3) coherent synchrotron radiation. The collision performance was improved for the head-on collision at high beam-beam parameter $\xi > 0.05$ in our simulations. Crab cavities make the condition of the head-on collision effectively for the finite crossing angle scheme of the beam-line arrangement. The crab cavity is expected to boost up the luminosity. Studies of the electron cloud and ion instabilities gave information of energy choice, which particles e^+ or e^- should be accumulated in high/low energy ring. In the present simulation, LER- e^+ option was slightly better than HER- e^+ option. Since this result may be delicate for the electron production parameters, careful studies are needed. In either case, it is important to be cured by ante-chamber, solenoids, etc. Coherent synchrotron radiation affects the bunch lengthening in the B factories. We have to solve how to treat the correlation length.

The author thanks fruitful discussions with S. Heifets, Y. Ohnishi, K. Oide, E. Perevedentsev, G. Stupakov, M. Tawada, K. Yokoya and F. Zimmermann.

REFERENCES

- [1] K. Akai et al., Nucl. Instrum. Meth. **A499**, 191 (2003).
- [2] K. Ohmi, Proceedings of EPAC2000, 433 (2000).
- [3] K. Hirata, Phys. Rev. Lett., **74**, 2228 (1995).
- [4] "KEKB B-factory design report", KEK Report 95-7 (1995).
- [5] K. Hirata, M. Zobiv, proceedings of EPAC96, 1158 (1996); M. Zobov et al., Frascati Phys. Ser. 10, 303 (1998).
- [6] K. Ohmi, K. Hirata and K. Oide, Phys. Rev. **E49**, 751 (1994).
- [7] K. Oide, K. Yokoya, Phys. Rev. **A40**, 315 (1989).
- [8] K. Ohmi, Phys. Rev. **E62**, 7287 (2000).
- [9] T. Chen, J. Irwin, R. Siemann, Phys. Rev. **E49**, 2323 (1994).
- [10] J. Irwin, private communications.
- [11] D. Shatilov, KEK-report, 96-14 (1994).
- [12] K. Ohmi, Phys. Rev. Lett. **75**, 1526 (1995).
- [13] M. Furman, G.R. Lambertson, Proceedings of MBI97 (KEK Report No. 97-17,1997), p. 170.
- [14] F. Zimmermann, see CERN ECLLOUD web page.
- [15] K. Ohmi, F.Zimmermann, Phys. Rev. Lett., **85**, 3821 (2000).
- [16] G. Rumolo, *et al.*, Proceedings of PAC2001,
- [17] K. Ohmi, Proceedings of PAC2001,
- [18] Y. Cai, Proceedings of ECLLOUD2002.
- [19] T.O. Raubenheimer, F. Zimmermann, Phys. Rev. **E52**, 5487 (1995).
- [20] K. Ohmi, Phys. Rev. **E55**, 7550 (1997).
- [21] S. Heifets, Proceedings of MBI97 (KEK Report No. 97-17,1997), p. 98.
- [22] E. Keil and W. Schnell, CERN Report TH-RF/69-48 (1969); D. Boussard, CERN Lab II/RF/Int 75-2 (1975).
- [23] G. Stupakov, S. Heifets, Phys. Rev. ST-AB., **5**, 054402, (2002).
- [24] K. Yokoya, private communications.
- [25] J.B. Murphy, S. Krinsky, R.L. Gluckstern, Part. Accel. **57**, 9 (1997).
- [26] Y.S. Derbenev *et al.*, DESY Report No. TESLA-FEL 95-05, 1995.
- [27] R.L. Warnock, SLAC Report No. SLAC-PUB-5375, 1990.